

A Non-Dimensional Approach to the Static and Vibratory Loading of Footings

L. L. KONDNER and R. J. KRIZEK, respectively, Instructor of Civil Engineering, The Johns Hopkins University, Baltimore, Md.; and formerly Research Assistant, The Johns Hopkins University, presently Instructor of Civil Engineering, The University of Maryland, College Park

An investigation of the surface deformations of rigid footings on homogeneous, cohesive soils under vertical static and vibratory loadings which is based on the methods of dimensional analysis in conjunction with small-scale model studies is reported. The physical quantities included are the strength and energy dissipation characteristics of the soil, the geometry of the footing, the magnitude of the static and dynamic loading, and the effects of frequency and amplitude of vibration. Practical illustrative examples are worked using the methods and data reported in this paper and the solutions are compared with those obtained for the conventional methods given by Housel, Kogler and Scheidig, and numerous authors in the field of soil mechanics.

THE BASIC PURPOSE of this paper is to report the results obtained from a small-scale laboratory investigation of the vertical static and vibratory loading of frictionless rigid footings on the surface of a homogeneous cohesive soil. Because the study is based on the methods of dimensional analysis and the results are presented in non-dimensional form, the results can be expected to hold for similar full-scale studies, provided all of the important variables have been included in the dimensional analysis and there is similitude between the corresponding non-dimensional parameters of the model and prototype. Thus, the seemingly impossible task of modeling is avoided. It must be recalled that dimensional analysis and model analysis are quite different, with dimensional analysis being a much more powerful and fundamental tool. Because of the complexity of soil as a structural material and the difficulty of soil problems in general, it is felt that a more extensive use of the methods of dimensional analysis will contribute to the field of soil mechanics.

Although some quantitative results are given, the results presented in this paper are intended to be qualitative indications of the possible results obtained using dimensional analysis as an experimental guide in problems in soil mechanics. The methods of dimensional analysis have been very successful in the field of hydraulics but their use in soil mechanics has been very limited, possibly because of the influence of boundary conditions, the water table, and the non-homogeneity and stratification of soils. The senior author intends to extend the present study to include the effects of stratification, eccentricity of loading, friction between the footing and the soil, single impulse loading, and the influence of a rigid ledge below the soil mass for both cohesionless and cohesive soils. It is felt that these difficult conditions can also be handled with the methods of dimensional analysis.

THEORETICAL CONSIDERATIONS

The methods of dimensional analysis as used to determine relationships among physical quantities which can be related by an equation are illustrated in a detailed manner in a companion paper by Kondner (12) on the static and vibratory cutting and penetration of soils.

The following physical quantities using the force-length-time system of fundamental units have been selected for use in the dimensional analysis:

- x = sinkage (contact deformation or surface settlement), L;
 t = time, T;
 F_T = total applied force, F;
 F_S = static force, F;
 ω = forcing frequency, T^{-1} ;
 p = natural frequency, T^{-1} ;
 τ = maximum unconfined compressive strength of the soil, FL^{-2} ;
 η = viscosity of soil, $FL^{-2}T$;
 ρ = mass density of soil, $FL^{-4}T^2$;
 g = acceleration of gravity, LT^{-2} ;
 A = cross-sectional area of footing, L^2 ;
 c = perimeter of footing, L; and
 a = amplitude of vibration, L.

A discussion of the foregoing physical quantities is included in the paper previously mentioned (12).

Since there are 13 physical quantities and 3 fundamental units, there must be 10 independent, non-dimensional π terms. These π terms can be methodically obtained by choosing three physical quantities, which contain all three fundamental units and cannot be formed into a π term by themselves (for example, F_T , ω , and τ), and combining them with each of the remaining quantities, one at a time.

There is nothing unique about the form of the non-dimensional terms obtained; hence it is possible to algebraically transform them so long as the final π terms are non-dimensional and independent. Because of the great difficulty in experimentally determining the exact nature of the function F , the π terms obtained, by the method indicated, were algebraically manipulated into the following non-dimensional parameters. In this study the sinkage (x) is considered the dependent variable and hence occurs in only one π term.

$$\begin{aligned}
 \pi_1 &= \frac{x}{c} & \pi_7 &= \omega t \\
 \pi_2 &= \frac{F_T}{A\tau} & \pi_8 &= \frac{g}{a\omega^2} \\
 \pi_3 &= \frac{c^2}{A} & \pi_9 &= \frac{\omega}{p} \\
 \pi_4 &= \frac{F_T}{F_S} = 1 + R & \pi_{10} &= \frac{g\rho}{\tau} \sqrt{\frac{F_T}{\tau}} \\
 \pi_5 &= \frac{a}{c} \\
 \pi_6 &= \frac{\omega\eta}{\tau} \text{ or either of the convenient forms } \frac{\tau t}{\eta} \text{ and } \frac{F_T t}{A\eta}
 \end{aligned} \tag{1}$$

The functional relationship among the various physical quantities can therefore be expressed as

$$x = c \Psi \left(\frac{F_T}{F_S}, \frac{F_T}{A\tau}, \frac{c^2}{A}, \frac{a}{c}, \frac{\omega\eta}{\tau}, \frac{c\omega}{g\tau}, \frac{\omega}{\rho}, \omega t, \frac{g\rho}{\tau}, \sqrt{\frac{F_T}{\tau}} \right) \tag{2}$$

The interpretations of the non-dimensional terms are similar to those given by the senior author for the static and vibratory cutting and penetration of cohesive soils (12)

By dropping from the study the π terms containing p and ρ (12), Eq. 2 can be reduced to the form

$$x = c \psi' \left(\frac{F_T}{F_S}, \frac{F_T}{A\tau}, \frac{c^2}{A}, \frac{a}{c}, \frac{\omega\eta}{\tau}, \frac{c\omega}{gt}, \omega t \right) \quad (3)$$

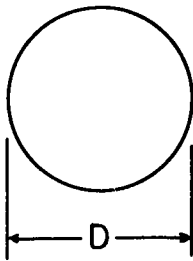
which is assumed to have a solution in an eight-dimensional space.

Although the natural frequency has been dropped from the functional relationship, it will be discussed qualitatively later in the paper. When comparing the relationship between any two π terms, the remaining π terms must not be forgotten. It must be noted that it is the value of the π term that is important and not its individual parts. Thus, the value x/c should be unique for constant fixed values of π_1 although the individual physical quantities composing the π terms may change.

EXPERIMENTAL APPARATUS

Model Footings

The model footings used in the study are shown in Figures 1 and 2. They include a set of six circular footings of various diameters, a square footing, four rectangular footings, and a special footing in the form of a symmetric cross. The circular footings have cross-sectional areas of 0.5, 1.0, 1.5, 2.0, 2.5 and 3.0 sq in. and a value of c^2/A equal to 4π which is a constant for all circular footings and the geometric minimum value for c^2/A . The square footing has a cross-sectional area of 2 sq in. and a value of c^2/a equal to 16 which is a constant for all square footings. The rectangular footings and the cross-shaped footing all have constant cross-sectional areas of 2 sq in. but have variable values of c^2/A as shown in Figure 2. All of the model footings are made of aluminum and have a polished finish.



$$\frac{c^2}{A} = 4\pi$$

inches D	inches ² A	inches C
0.79	0.5	2.48
1.13	1.0	3.55
1.38	1.5	4.34
1.59	2.0	5.00
1.78	2.5	5.59
1.95	3.0	6.13

Figure 1. Circular footings.

Static Test Apparatus

The two types of static test apparatus used are shown in schematic form in Figures 3 and 4. As shown in Figure 3, the static weight is applied to the footing through a ball bearing with the use of a lever system consisting of a rigid arm pivoted at point e.

The apparatus in Figure 4 operates as follows. The load is applied to the footing through a ball bearing and a shaft by placing weights on the loading platform. The shaft is free to move vertically in the guides. The sinkage is measured with an indicator dial.

Vibratory Test Apparatus

The vibratory test apparatus is schematically shown in Figure 5. The load is ap-


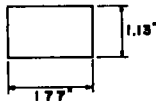
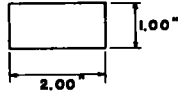
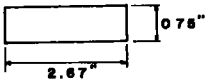
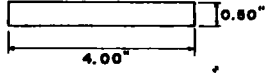
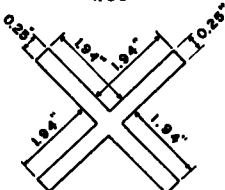
Footings	c	A	$\frac{c^2}{A}$
	5.66	2.0	16
	5.80	2.0	16.8
	6.00	2.0	18
	6.83	2.0	23.4
	9.00	2.0	40.5
	16.5	2.0	136

Figure 2. Footings of constant area and variable perimeter.

United Clay Mines Corporation. It is mined on US 40 approximately 6 miles north of Baltimore at Popular, Maryland. The deposit is a part of the Patapsco formation of the Potomac group which is of the lower Cretaceous period. The characteristics of the clay are as follows:

Liquid limit	42 %
Plastic limit	21 %
Plasticity index	21 %
Specific gravity	2.68
Optimum moisture content	15 %
Maximum dry density	114 pcf

(Modified AASHTO)

Test samples were prepared to approximately the desired unconfined compressive strengths by a compaction process using moisture-density-strength relationships previously obtained (11).

EXPERIMENTAL RESULTS

Static Tests

Since this was the first time, to the authors' knowledge, that small-scale model

plied to the footing through a ball bearing and a solid shaft which is connected in series with a dynamometer and static weights both of which are attached to the moving coil of the electro-magnetic exciter. When the shaft is not bearing on the footing, the weight acting on the moving coil is transferred by small, leaf springs to the field coil which is suspended on the guide track by counter weights. By use of the adjustment reel the shaft is brought to bear on the footing. The position reel is used to raise or lower the exciter along the guide track in order to maintain an average relative displacement of zero between the field coil and the equilibrium position of the moving coil and thus a constant resultant static force. The output of the exciter used was limited to a maximum sinusoidal dynamic force amplitude of 10 lb for a frequency range of 20 to 60 cycles per second.

Static and dynamic forces are measured by the electric dynamometer whose response is amplified and viewed on a cathode-ray oscilloscope. The amplitude of vibration is measured with a piezoelectric crystal-type accelerometer and a vibration meter calibrated to read in micro-inches. The sinkage of the footing is measured by means of an indicator dial calibrated in thousandths of an inch with a range of 1 in.

MATERIAL TESTED

The soil used to date in this investigation is a Jordan buff clay obtained from the

studies in conjunction with the methods of dimensional analysis had been used to investigate the loading of frictionless and rigid footings on the surface of a homogeneous cohesive soil, it was decided to first conduct experiments with only static loadings. Eqs. 1 and 3 show that the static load-sinkage relation can be expressed in the form

$$x = c \psi'' \left(\frac{F_T}{A\tau}, \frac{c^2}{A}, \frac{\tau t}{\eta} \right) \quad (4)$$

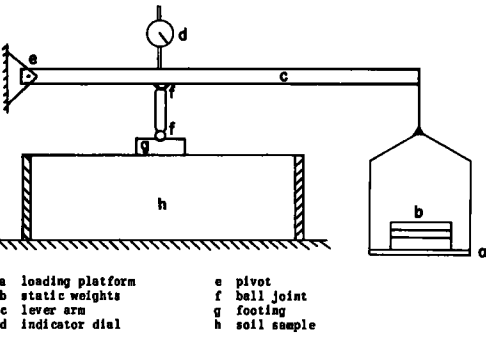


Figure 3. Schematic diagram of static apparatus.

The non-dimensional term $\tau t/\eta$ was obtained from Eq. 1 by dividing π_7 by π_6 .

Thus, Eq. 4 includes time effects which are known to be of great practical consequence. Those persons familiar with the use of rheological models in the field of high polymers will recognize the term η/τ as being proportional to the relaxation time for a Maxwell material and as being proportional to the retardation time of a Kelvin material. Thus, the non-dimensional term $\tau t/\eta$ controls the rate of sinkage in a static test. The present state of development of the field of soil mechanics is such that very little in a quantitative manner can be done with this term. The senior author has recently initiated an extensive research program into the static and dynamic viscoelastic properties of soils and is hopeful that considerable progress can soon be made in stress-strain-time phenomena in soils (11).

Pressure Intensity, Soil Strength and Shape Effects. — To illustrate the convergent nature of the non-dimensional form of presenting the experimental data, load-sinkage tests were conducted on a very soft sample using circular footings. The effects of the cross-sectional area on the sinkage of footings was evaluated by using different values of A while maintaining a constant value of c^2/A . For circular footings of any diameter the value of c^2/A is equal to 4π . Thus, such tests will give the relationship between the dependent variable (x/c) and $F_T/A\tau$ for $c^2/A = 4\pi$.

Figure 6 is a conventional plot of the load-sinkage data for the aforementioned tests. The same data are plotted in the non-dimensional form of x/c versus $F_T/A\tau$ in Figure 7. It is important to note that the rate of loading for all of these tests was 1 kg per min with sinkage readings being taken at the end of the 1 min intervals. Although the load application rate was constant, the rate of stress application was not constant because of the difference in cross-sectional area. The senior author's recent work in stress perturbations about various stress levels indicates that the viscous response of the soil being studied is a function of the stress level; thus, the viscous nature of the soil is non-Newtonian and the time effects should be different

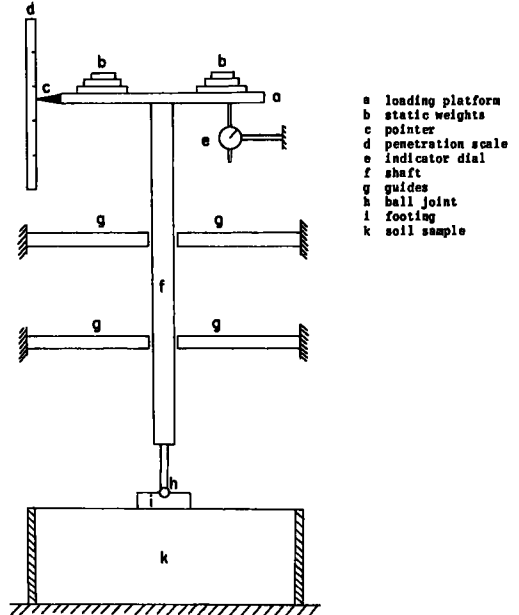


Figure 4. Schematic diagram of static apparatus.

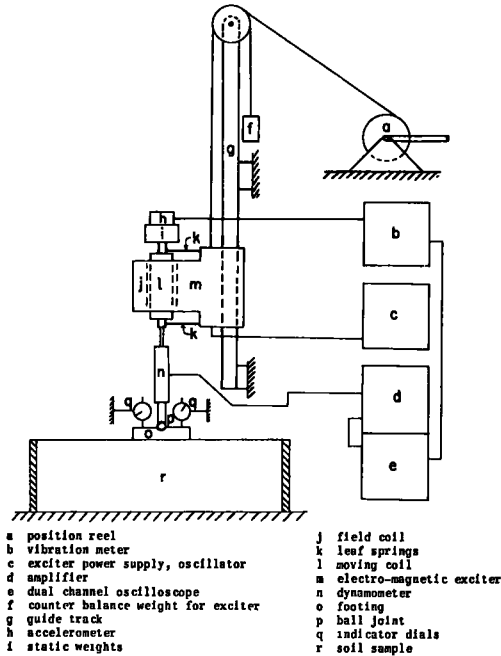


Figure 5. Schematic diagram of vibratory apparatus.

for the different footings. This means that to obtain a unique relationship between x/c and $F_T/A\tau$ a constant value of $\tau t/\eta$ would have been required for all of these tests. Theoretically, this could have been done by varying the loading rate for each test either by varying the load interval or by changing the time interval of loading. Unfortunately, the field of soil mechanics has not yet reached a state of development where such loading rates can be predicted. It may be that a reverse process could be used to investigate such viscous phenomena. Thus, the "scatter" in Figure 7 is probably due to viscous effects as well as experimental error.

Theoretically, the same curve of x/c versus $F_T/A\tau$ could be obtained by varying the value of τ for any one of the circular footings provided the remaining π terms are kept constant and equal to their values in the previous tests. Figure 8 is the result of such tests conducted on a stiff sample using the same loading rate as in the previous tests. Once again variations in the term $\tau t/\eta$ seem to prevent a complete agreement with the results of Figure 7.

If term $\tau t/\eta$ had been kept constant in the foregoing tests, the results obtained

would have been expected to hold in the field. For circular cross-sections the only field data that was located is that reported (4) on the presentation of rigid plate bearing test data. Load versus sinkage data of subgrade for plate diameters ranging from 1 to 7 ft (4, Tables 3 and 5) have been plotted in non-dimensional form in Figure 9. The value of the unconfined compressive strength which was used was estimated from another paper connected with the same study (5). Figure 9 shows a surprisingly small amount of scatter for the wide range of plate sizes and pressures used. When compared with Figures 7 and 8, the best agreement is obtained with Figure 8. The results given in Figure 8 were obtained for a "stiff" soil sample having an unconfined compressive strength closer to that of the field tests. Therefore the viscous effects are less when comparing Figures 8 and 9 than when comparing Figures 7 and 9. The generally good agreement obtained from the non-dimensional plots for the wide range of cross-sectional areas, soil strengths and applied loads seems very encouraging.

To obtain the variation of the sinkage (x/c) as a function of c^2/A , a series of tests were conducted on footings of equal cross-sectional area but with different values of c^2/A for soil samples having approximately the same unconfined compressive strengths. The range of c^2/A tested was from the geometrical minimum of 4π for circular footings to a value of 136 for the cross-shaped footing of Figure 2. The results of these tests are given in Figures 10 and 11. Figure 10 is a plot of x/c versus $F_T/A\tau$ for various values of c^2/A . Figure 11 is a plot of x/c versus c^2/A for various values of $F_T/A\tau$. For a constant value of $F_T/A\tau$, the sinkage parameter (x/c) increases as c^2/A decreases. Thus, for a constant cross-sectional area, a circular-shaped footing has the most undesirable sinkage characteristics.

The results of Figures 7, 8, 9, 10, and 11 are in agreement with the observations on size effects reported by Taylor (15) and Tschebotarioff (18).

It must be recalled that the foregoing data were obtained from carefully controlled tests on homogeneous cohesive soil in which any eccentricities of loading were carefully avoided. Thus, the failure mechanism was such that failure occurred by a gradual sinkage without any tipping of the footing. In actual field studies the soil deposit may

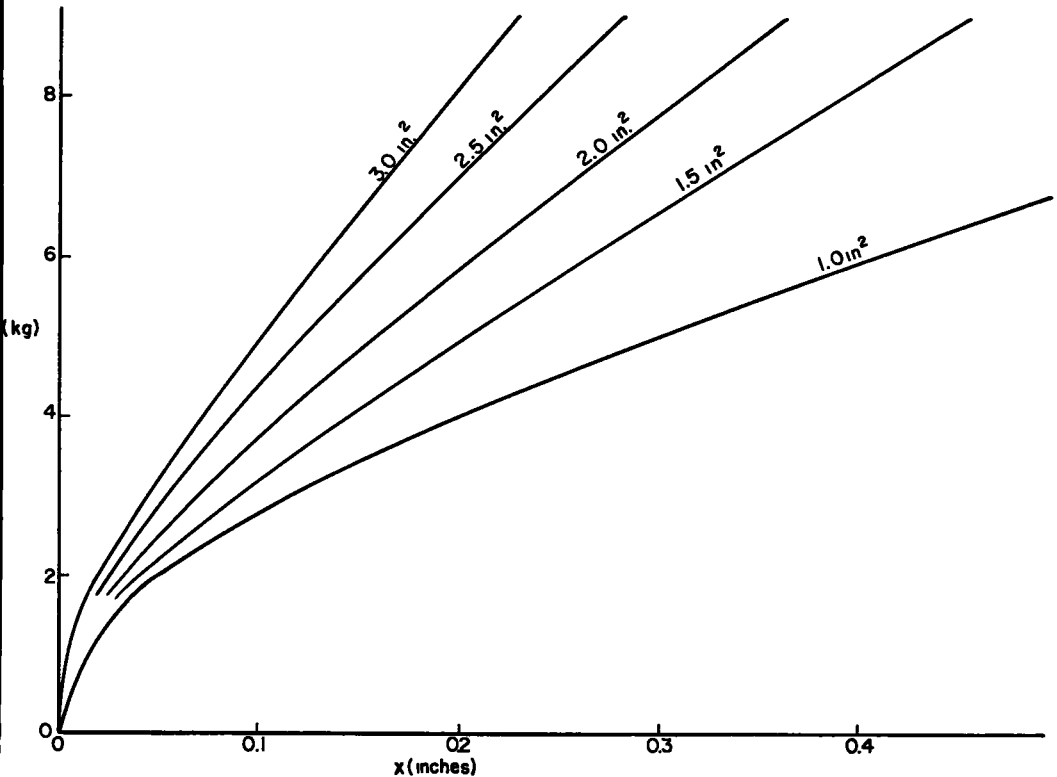


Figure 6. Sinkage versus load: circular footings.

not be homogeneous and the eccentricities may be considerable, thus inducing different failure mechanisms for different cross-sectional shapes of constant area. There are two different phenomena to be considered; namely, the sinkage characteristics as indicated by Figure 11 and the stability characteristics which may be a function of the homogeneity of the cohesive soil and both the shape of the footing and the magnitude of the load eccentricity.

Load History and Creep Effects. — To get some qualitative indication of the importance of time effects on the study, a series of load history and creep tests were conducted on soft samples using a circular footing with a cross-sectional area of 2 sq in. The selection of a circular footing and a soft soil was to accentuate viscous effects through large sinkages and to increase stability against tipping of the footing.

The results of the creep tests for various stress levels are given in Figure 12 in the form of x/c versus t . Since the ratio of τ/η is approximately constant for any one creep test but not for different creep stress levels (non-Newtonian effects), the time t is approximately proportional to the non-dimensional term $\tau t/\eta$. Thus Figure 12 can be considered as giving in a qualitative manner the variation of x/c with $\tau t/\eta$ for different values of $F_T/A\tau$ and a constant value of $c^2/A = 4\pi$.

The slopes of these curves for various stress levels at constant times are an indication of the manner in which the strain rate varies as a function of the applied stress level. This indicates that the strain rate increases with the increase in stress level in a non-linear manner. Thus, the viscous response is non-Newtonian. The rate at which the strain rate is increasing with increase in stress level indicates a quasi-Bingham behavior (Fig. 13) for the soil being studied. This agrees with the senior author's preliminary results on the dynamic viscoelastic properties of the clay in question as reported to the U. S. Army, Corps of Engineers (11).

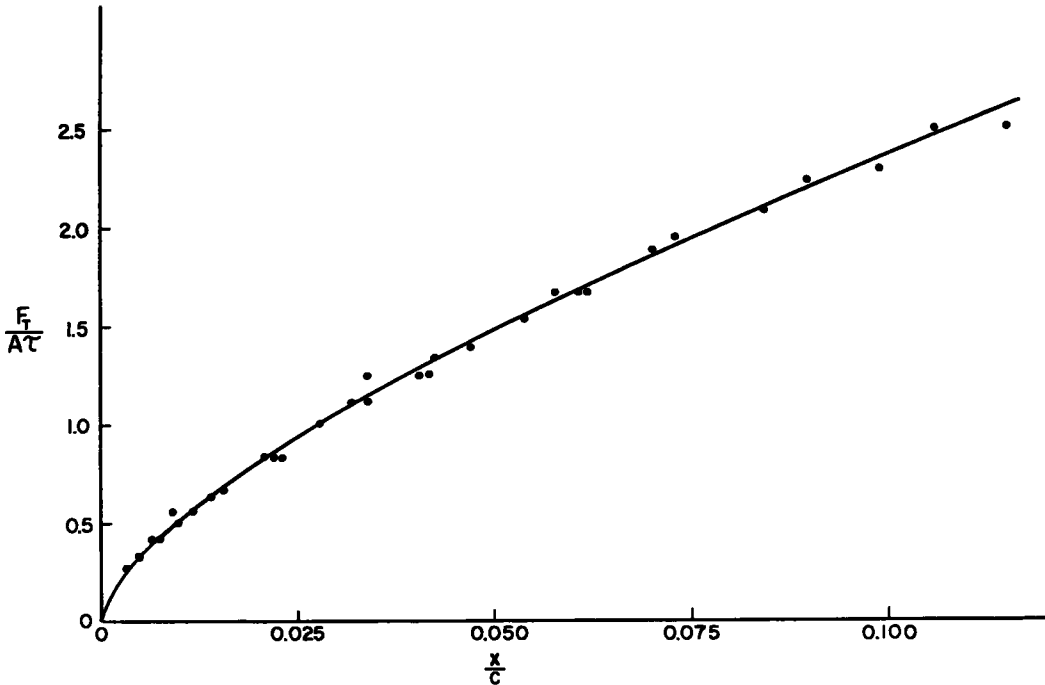


Figure 7. Non-dimensional plot for circular footings of x/c versus $F_T/A\tau$.

Figure 13 illustrates several kinds of viscous behavior. A Newtonian material has a linear relationship (from the origin) between stress and strain rate while non-Newtonian is any other curve. Bingham response is also linear but flow does not develop until a yield stress is reached. Note that the linear relationships mean a constant viscosity. The actual response of the soil considered is non-linear and each stress level is associated with a different viscosity.

The results of the tests conducted with different load histories are shown in Figure 14. The loading sequences used for these tests were 0.5 kg per min, 1.0 kg per 2 min, 2.0 kg per 4 min, and 4.0 kg per 8 min. Thus, for all of the tests, the average loading rate was 0.5 kg per min and the average rate at which the applied stress was being increased was 0.55 psi per min. A comparison of the values of x/c for times of 8 min and 16 min shows an increase in x/c for an increase in the loading sequence. A check of the unconfined compressive strengths showed that the larger load sequences were run on soils with slightly lower values of τ and consequently lower values of η . Since the applied stresses were equal at these times and the viscosity is lower for the larger load sequences, the strains for the larger load sequences should be greater. This agrees with the larger values of x/c for the larger load sequences even though the average rate of stress increase was constant.

Although this study is primarily concerned with the rheologic characteristics (referred to by many as plastic, viscous, or secondary time effects) and not with "consolidation" phenomena, the results of this section agree with those obtained for consolidation studies. For the soil tested the smaller increments of load and hence the correspondingly larger number of increments gave smaller surface deformations. When the load is applied gradually the soil skeleton has time to reorient itself and hence to develop a greater resistance to the next increment of load than would be the case if a larger increment of load was applied.

The different results given in Figures 7, 8, 9, 12 and 14 can be reconciled by recalling that variations in τ and the applied stress F_T/A cause different changes in η

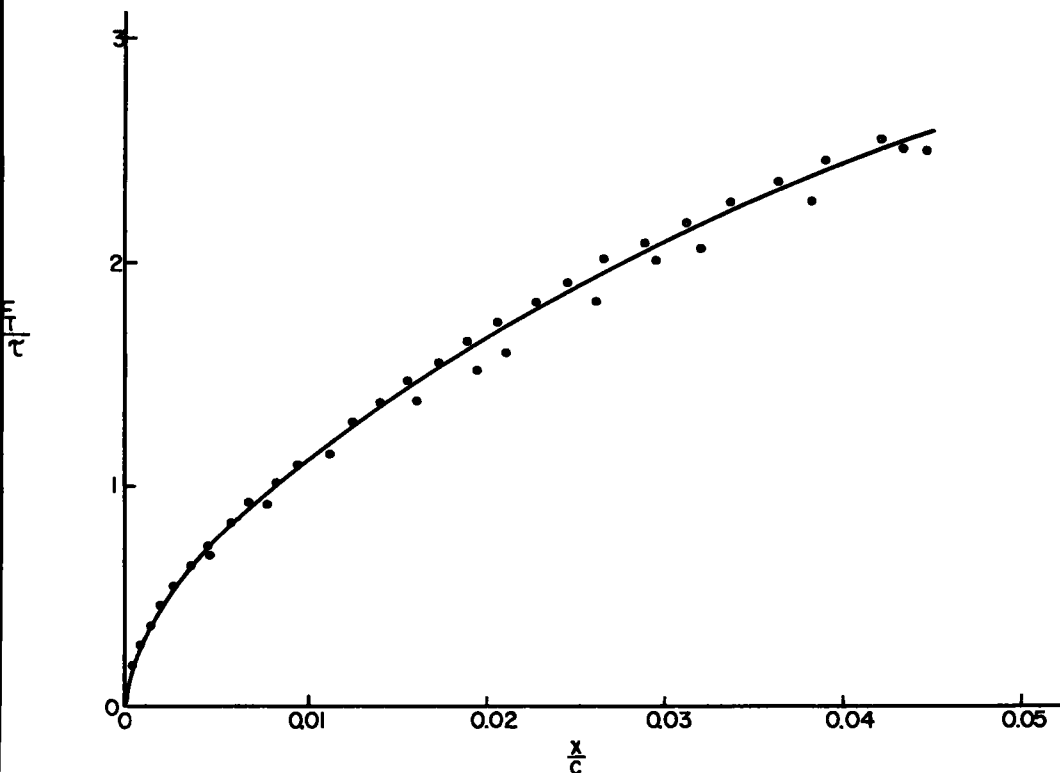


Figure 8. Non-dimensional plot for circular footings of x/c versus $F_T/A\tau$.

and that the various rates of stress application mean that different values of time should be used. Therefore the relationship between (x/c) and $F_T/A\tau$ for different size footings under different rates of stress application on cohesive soils having various unconfined compressive strengths will not be a unique relation until the non-dimensional parameters c^2/A and $\tau t/\eta$ or its equivalent expression $F_T t/a\eta$ are maintained constant.

Practical Applications

The authors believe that the methods of dimensional analysis offer considerable promise in the transformation from model studies to prototype response. To illustrate some of the possible applications of the results presented, several practical problems are solved using the methods presented and the solutions are compared with the solutions obtained using conventional methods of analysis. In this section the viscous effects expressed by the term $\tau t/\eta$ are neglected and it is assumed that Figures 10 and 10-a can be used to obtain the surface deformations under a rigid footing of a homogeneous, cohesive clay mass of any consistency as a function of the total applied vertical load regardless of the cross-sectional area of the footing for a variety of cross-section shapes. Figure 10-a is an enlarged detailed plot of the experimental data near the origin in Figure 10 for square footings.

Specific Problems. — Example A: Comparison with the Housel Method. The following example is taken from Andersen (1, p. 81). It is desired to design a square footing to transmit a load of 94 kips to a cohesive soil without exceeding a settlement of $\frac{1}{2}$ in. Two tests are made with bearing areas of 1 ft by 1 ft and 2 ft by 2 ft; they give settlements of $\frac{1}{2}$ in. for loads of 7,600 and 20,800 lb, respectively.

The solution by the Housel method gives the desired footing having a side length equal to 5 ft.

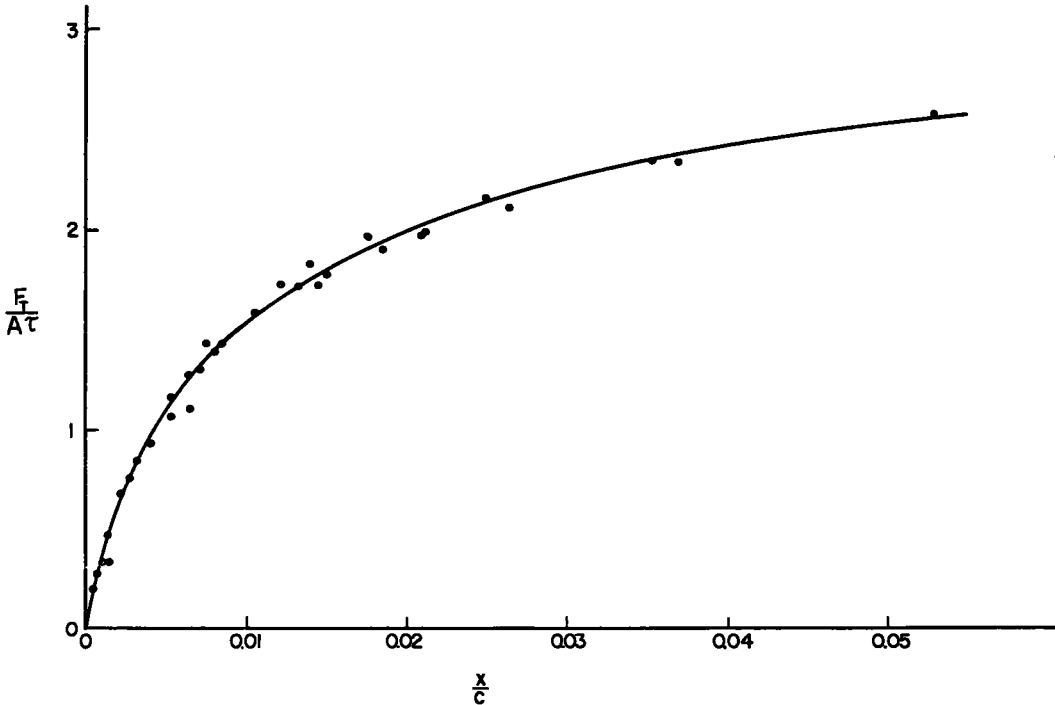


Figure 9. Non-dimensional plot of field data: x/c versus $F_T/A\tau$.

Using the non-dimensional method as expressed in Figure 10-a, the solution is as follows:

For the 1- by 1-ft test plate

$$\frac{F_T}{A\tau} = \frac{7600}{1\tau} \quad \text{and} \quad \frac{x}{c} = \frac{0.5}{48} = 0.01042$$

Entering Figure 10-a with $x/c = 0.01042$, one obtains a value of $F_T/A\tau = 0.614$. The value of τ is obtained by equating the two values of $F_T/A\tau$. Inasmuch as the τ for the test plate and the footing is the same, this value is then substituted into the prototype expression and

$$\frac{F_T}{A\tau} = \frac{94,000 \times 0.614}{7,600 b^2} = \frac{7.6}{b^2} \quad \text{and} \quad \frac{x}{c} = \frac{0.5}{48b}$$

With the use of Figure 10-a the solution of the two equations is easily obtained by trial and error to be $b = 4.93$ ft.

The same process can be used for the 2- by 2-ft test plate to obtain a solution of $b = 5.01$ ft.

The non-dimensional method required the data from only one load test. The agreement between the Housel and the non-dimensional method is excellent.

Example B: Comparison with the Housel Method. A second problem was selected from Andersen (1, p. 85, No. 4).

It is desired to design a square footing to transmit 328 kips to a cohesive soil without exceeding a settlement of $\frac{1}{2}$ in. Two tests are made with bearing areas of 1 ft by 1 ft and 2 ft 3 in. by 2 ft 3 in. They gave $\frac{1}{2}$ in. settlements for 7,600 lb and 25,000 lb respectively.

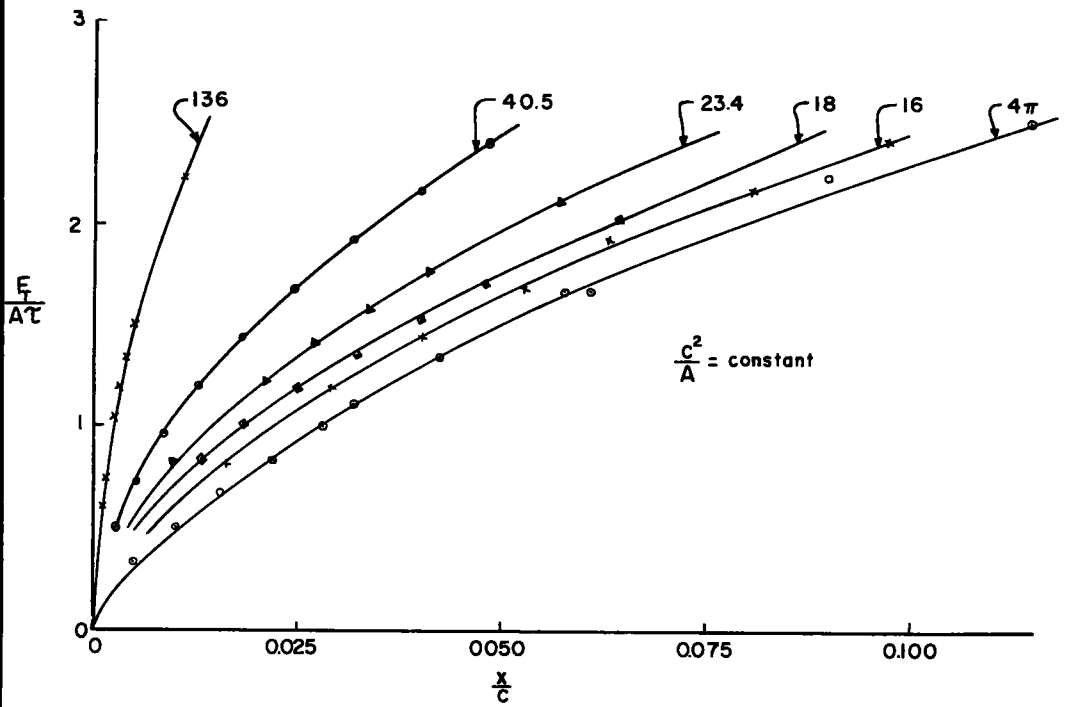


Figure 10. Non-dimensional plot of x/c versus $F_T/A\tau$ for constant values c^2/A .

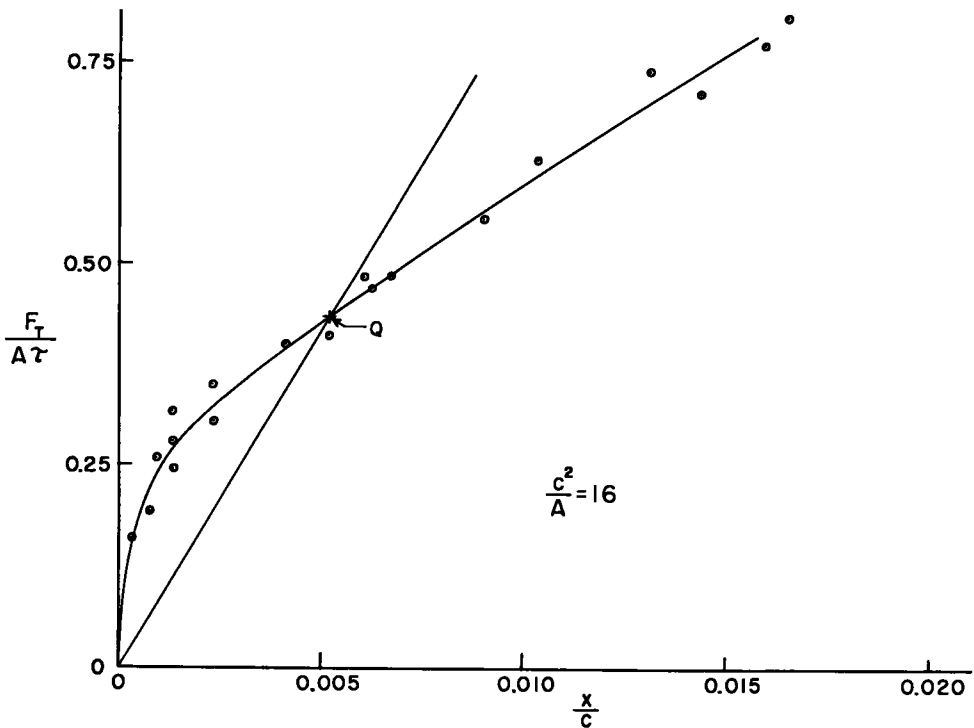


Figure 10-a. Non-dimensional plot for square footings.

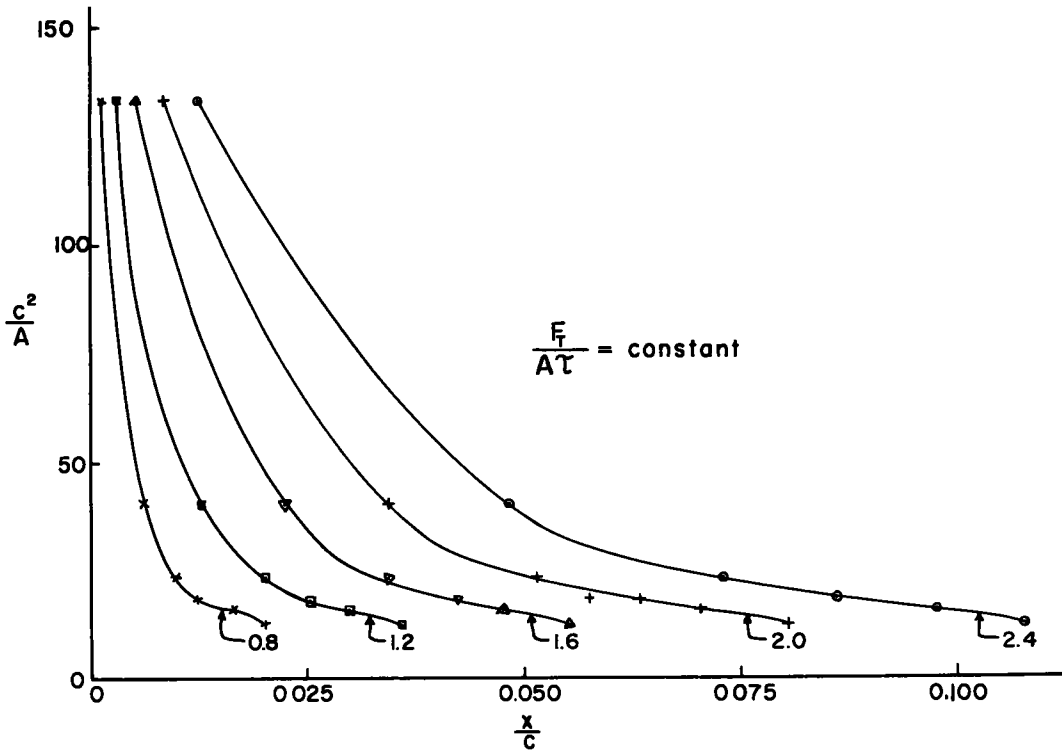


Figure 11. Non-dimensional plot of x/c versus c^2/A for constant values of $F_T/A\tau$.

The solution by the Housel method is $b = 10$ ft and by the non-dimensional method, as previously illustrated, is approximately 10.4 ft. The agreement for this example is also fairly good.

Example C: Proportioning Footings to Prevent Differential Settlement. The foundation designer is frequently required to design spread footings for a structure such that harmful differential settlements are prevented. It is well known that footings of different sizes will settle unequally even though they carry the same unit pressure intensity. The following problem is taken from Andersen (1, p. 84) where it is solved by the method of Kogler and Scheidig.

It is desired to find the square contact areas for three single footings carrying, respectively, 36, 48, and 72 kips. The compressible layer in which the footings are resting extends 6 ft below the contact areas. It is assumed that a square footing of 9 sq ft will be used for the load of 36 kips and the other footings will be proportioned so that the final deflections will be approximately equal for the three loads.

The solutions given by Andersen using the Kogler and Scheidig method are

- $b = 3$ ft for the 36-kip load,
- $b = 3.66$ ft for the 48-kip load, and
- $b = 4.92$ ft for the 72-kip load.

The solution obtained using the non-dimensional method is as follows. Because all three footings are on the same soil and the settlements are to be equal, the soil properties should not affect the solution. The 3-ft by 3-ft footing carrying the 36-kip load will be used in the same manner as the test plates in Examples A and B. Inasmuch as the settlement of the 3-ft by 3-ft footing is unknown, a value may be assumed (for example $\frac{1}{8}$ in.).

$$\frac{x}{c} = \frac{0.5}{144} = 0.00347 \quad \text{and} \quad \frac{F_T}{A\tau} = \frac{36000}{9\tau}$$

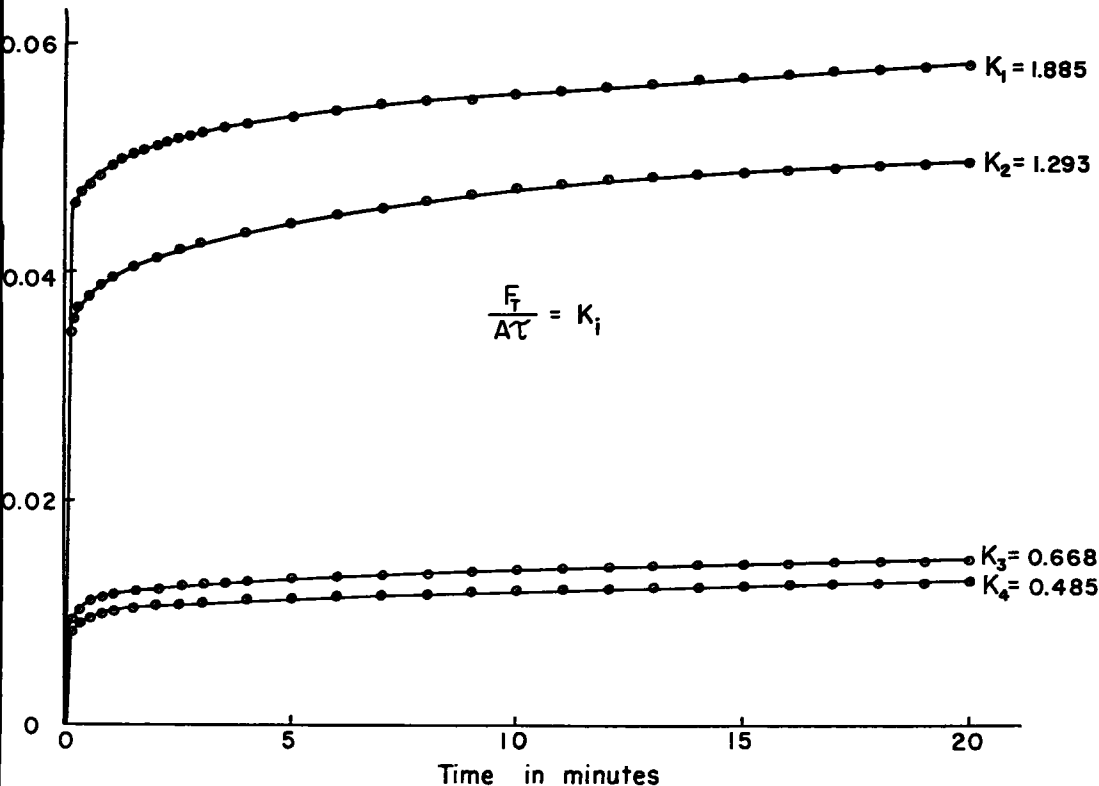


Figure 12. Static creep tests.

For $x/c = 0.00347$ Figure 10-a gives $F_T/A\tau = 0.37$. Following the procedure of illustrative Example A gives for the other two loading conditions

$$\frac{F_T}{A\tau} = \frac{4.45}{b^2} \quad \text{and} \quad \frac{x}{c} = \frac{0.5}{48b} \quad \text{for the 48-kip load,}$$

and

$$\frac{F_T}{A\tau} = \frac{6.67}{b^2} \quad \text{and} \quad \frac{x}{c} = \frac{0.5}{48b} \quad \text{for the 72-kip load.}$$

These two sets of equations can be solved by trial and error to give

$b = 3.58$ ft for the 48-kip load, and

$b = 4.56$ ft for the 72-kip load.

The solutions were repeated using assumed settlements of 1 and 2 in. with the following results:

For an assumed settlement of 1 in., b was equal to 3.58 ft and 4.67 ft for the 48-kip and 72-kip loads, respectively, while b was 3.66 ft and 4.87 ft, respectively, using an assumed settlement of 2 in.

It must be noted that the Kogler and Scheidig method was developed to include the depth of the soil to a rigid ledge. The senior author has not yet extended the non-dimensional method to include this condition although it should be done in the near future. In spite of this difficulty the largest discrepancy (assumed settlement of $\frac{1}{2}$ in. for 72-kip load) was only 7.3 percent. If one considers the location of the 10 percent pressure bulb as a function of the length of the side of the footing and with regard to the depth of

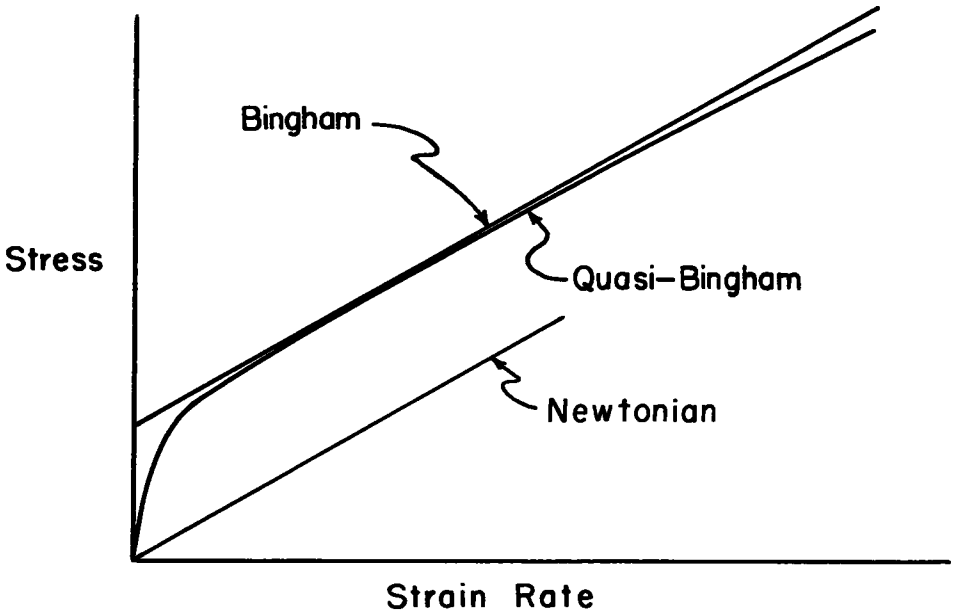


Figure 13. Bingham and quasi-Bingham material.

the soil layer given, such a small percent error is to be expected for the 48-kip load but a somewhat larger error would be expected for the 72-kip load.

Limited Generalizations. — The following are some generalizations obtained from the non-dimensional method.

Non-Linear Case. For a constant cross-sectional shape and a constant value of $F_T/A\tau$ (that is, for a constant applied pressure and the same soil), a constant value of x/c will be obtained regardless of the total load and the cross-sectional area. This does not involve any assumption regarding the linearity of the load versus surface deformation relationship. Therefore, under these conditions

$$\frac{x}{c} = \text{constant} = k.$$

For circular footings

$$\frac{x}{c} = \frac{x_1}{\pi d} = \frac{x_2}{\pi d_2} \quad \text{or} \quad \frac{x_1}{x_2} = \frac{d_1}{d_2} \quad (5)$$

This agrees with observations attributed to Terzaghi by Andersen (1). For square footings

$$\frac{x}{c} = \text{constant} = k_2 = \frac{x_1}{4 b_1} = \frac{x_2}{4 b_2}$$

or

$$\frac{x_1}{x_2} = \frac{b_1}{b_2} \quad (6)$$

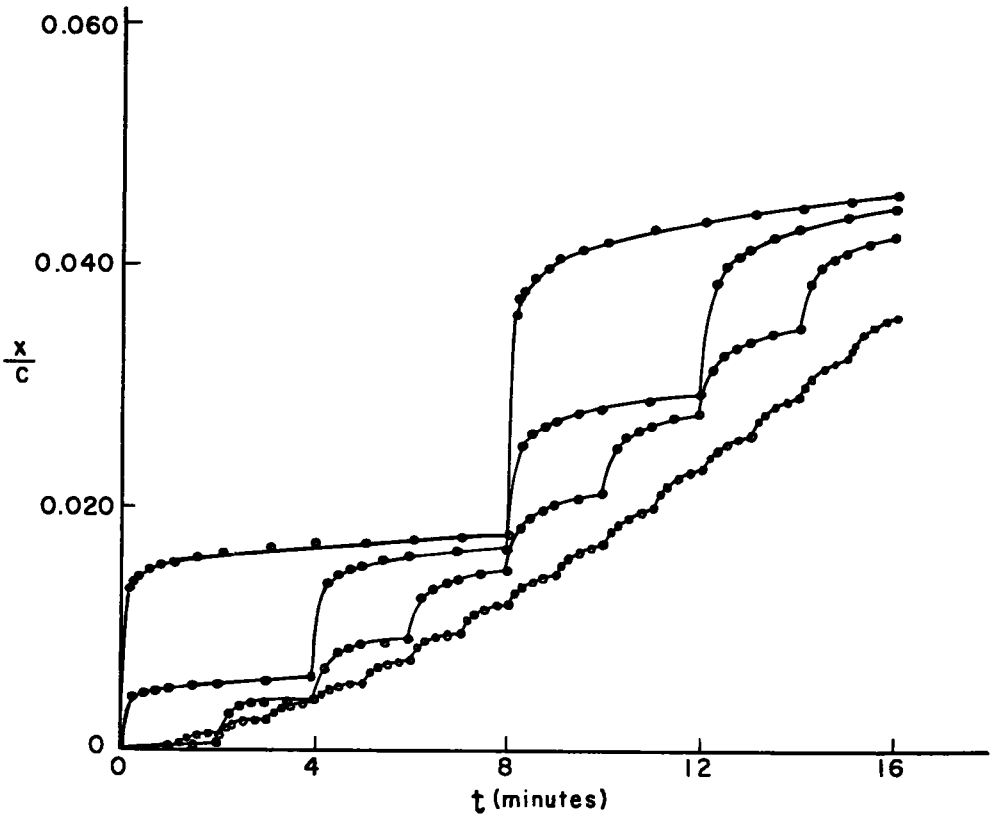


Figure 14. Load history tests.

For rectangular footings

$$\frac{x}{c} = \text{constant} = k_s = \frac{x_1}{2b_1(1+a)} = \frac{x_2}{2b_2(1+a)}$$

or

$$\frac{x_1}{x_2} = \frac{b_1}{b_2} \quad (7)$$

in which a is the ratio of the length to the width of the footing and is a constant for both footings.

Linear Case. If one assumes an initially linear load versus settlement relationship, as numerous authors do (14, Fig. 5: 18-b, p. 128), then the relationship for $F_T/A\tau$ versus x/c for a constant value of c^2/A can be written as:

$$\frac{\left[\frac{F_T}{A\tau} \right]_M}{\left[\frac{F_T}{A\tau} \right]_F} = \frac{\left[\frac{x}{c} \right]_M}{\left[\frac{x}{c} \right]_F} \quad (8)$$

in which subscripts M and F refer to the model (test plate) and the prototype footing, respectively. Note that for the linear assumption Eq. 8 can be used for any pressure

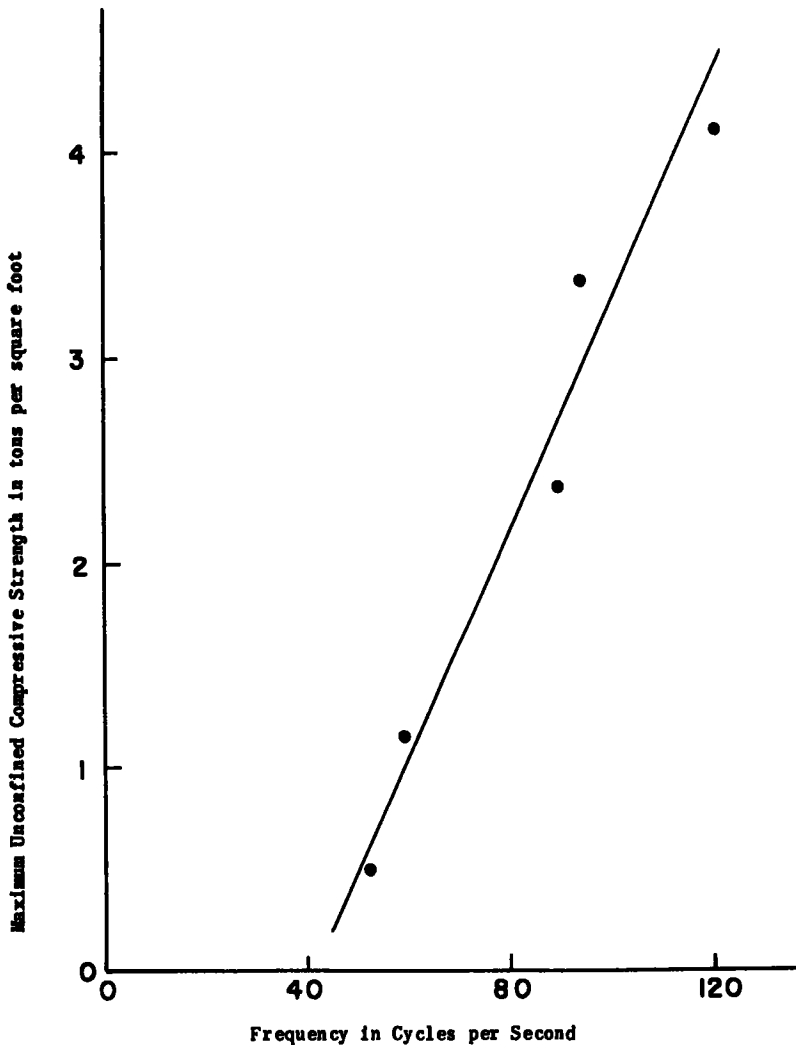


Figure 15. Natural frequency versus unconfined compressive strength.

intensity F_T/A . The validity of the linear assumption is discussed later. For constant pressure F_T/A and $\tau_M = \tau_F$ Eq. 8 reduces to Eqs. 5, 6 and 7 for circular, square, and rectangular footings, respectively. Various forms of Eqs. 5, 6, and 7 are given in the literature; for example, by Sowers and Sowers (14, Eq. 5: 12a, p. 129, and stated in words by others p. 583).

Discussion of Linearity. The following example illustrates some of the possible effects that the linearity assumption can have on the computed settlements.

A load test conducted on a clay with a 2- by 2-ft test plate gave a settlement of $\frac{1}{2}$ in. under a load of 12 kips. Estimate the surface settlement of an 8- by 8-ft rigid footing under a load of 128 kips.

It is important to note that the pressure intensities are 3 kips per sq ft and 2 kips per sq ft for the bearing plate and the footing, respectively. A first order approximate solution to this problem (which some people might use) would be to reduce the bearing plate data to that for a pressure intensity of 2 kips per sq ft (the same as that of the footing) by using the assumption of a linear relationship between the load and the surface settlement. Thus, for a pressure intensity of 2 kips per sq ft the bearing plate would

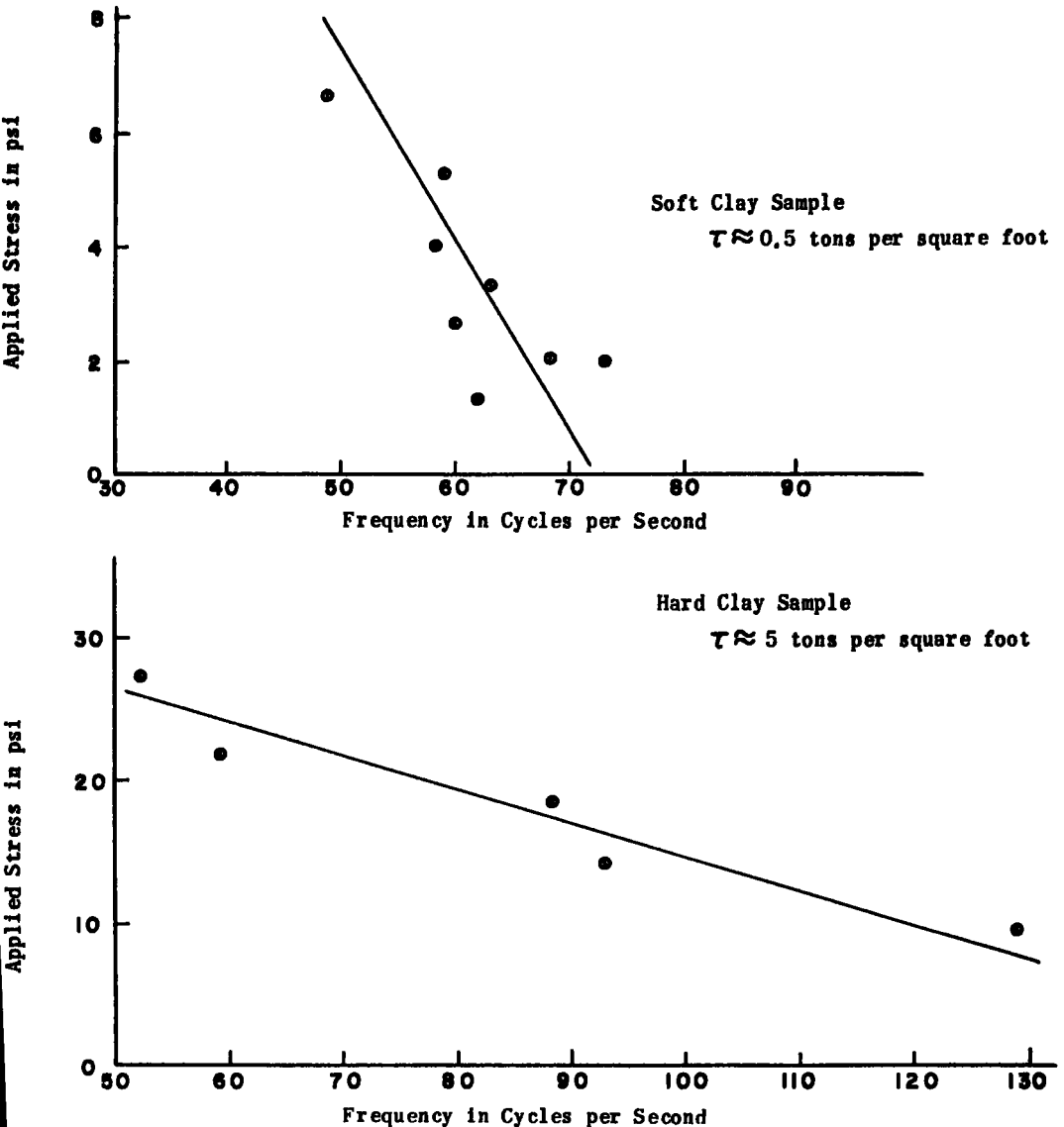


Figure 16. Natural frequency versus contact stress.

be assumed to give a surface settlement of $\frac{1}{3}$ in. Now that the pressure intensities are equal, Eq. 6 (14, Eq. 5: 12a, p. 129) could be used to obtain a prototype surface settlement of 1.33 in.

With the linear assumption the non-dimensional method as expressed by Eq. 8 gives

$$\frac{\frac{12}{4\tau}}{\frac{128}{64\tau}} = \frac{\frac{0.5}{2 \times 48}}{\frac{x}{8 \times 48}}$$

$$x = 1.33 \text{ in.}$$

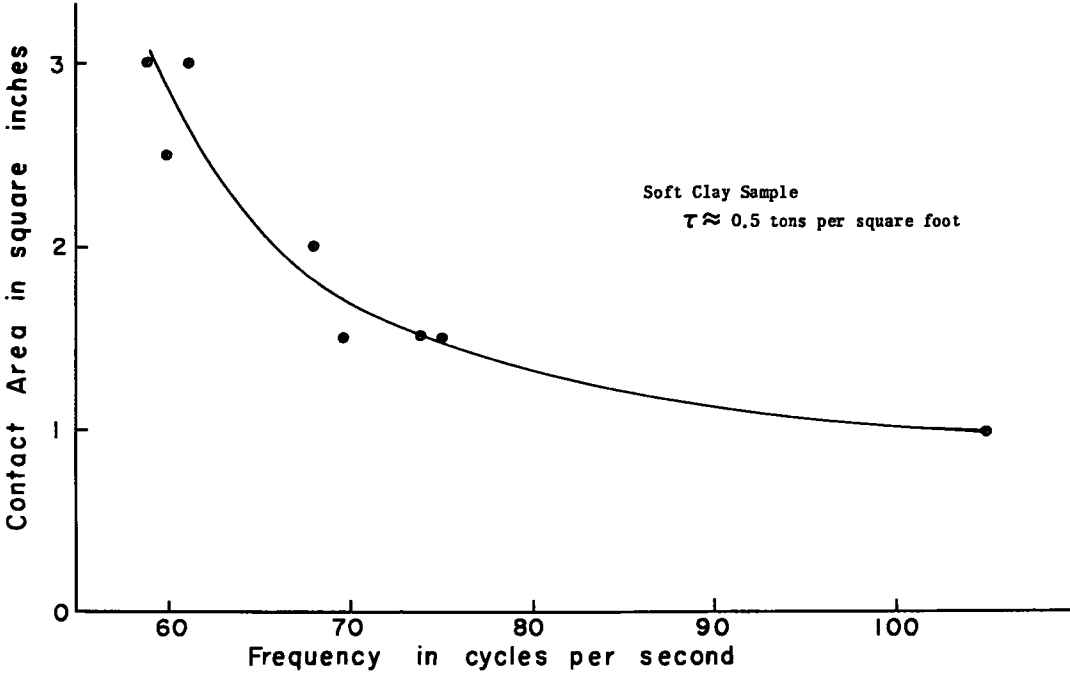


Figure 17. Natural frequency versus cross-sectional area for constant contact stress.

For comparison the same problem will be solved by the non-dimensional method without making the assumption of a linear load versus settlement curve. Neglecting the time effects, Figure 10-a for square footings may be considered to hold for any pressure intensity on a cohesive soil of any unconfined compressive strength.

From the load test data

$$\frac{F_T}{A\tau} = \frac{12000}{4\tau}$$

and

$$\frac{x}{c} = \frac{0.5}{2 \times 4 \times 12} = 0.00521$$

For a value of $x/c = 0.00521$, Figure 10-a gives

$$\frac{F_T}{A\tau} = 0.433 = \frac{12000}{4\tau}$$

Substituting for τ in the prototype footing gives

$$\frac{F_T}{A\tau} = \frac{128000 \times 4 \times 0.433}{64 \times 12000} = 0.2886$$

For

$$\frac{F_T}{A\tau} = 0.2886$$

Figure 10-a gives

$$\frac{x}{c} = 0.00164$$

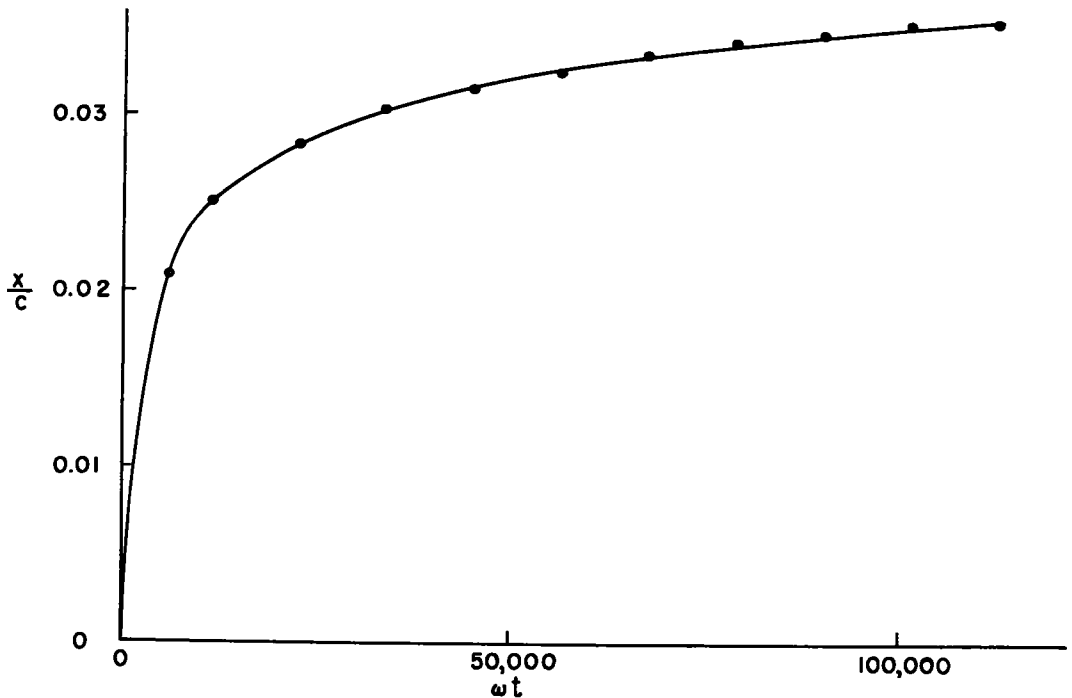


Figure 18. Dynamic creep curve.

Therefore

$$x = 0.00164 c = 0.00164 \times 4 \times 12 \times 8 = 0.63 \text{ in.}$$

which is only 47.4 percent of the surface settlement estimated with the linear assumption.

The reason for the smaller value of the surface settlement, as given by the non-dimensional data of Figure 10-a, when compared with that obtained for the linear assumption, is as follows. The data from the load test are actually only one point (point Q of Fig. 10-a) on the non-linear curve of $F_T/A\tau$ versus x/c . The linear assumption gives a straight line from the origin through point Q. Therefore, for pressure intensities less than that of the load test the surface settlement predicted by Figure 10-a will be less than that obtained with the linear assumption, while for pressure intensities greater than that of the load test, the predicted values will be greater than those for the linear assumption.

Experimental evidence indicates considerable non-linear behavior in cohesive soils. Therefore considerable caution should be exercised in the use of linear approximations and it should be realized that such linear approximations are only valid over a limited range of variables. Such limitations are clearly pointed out in the literature. For example, when writing on loading tests on cohesive soil Terzaghi (16) states "...we always find that the ratio between the settlement and the unit load increases with increasing load." Terzaghi (16) also states, "the increase of the rate of settlement under higher loads is due to the fact that soils do not obey Hooke's law."

Because of the great number of variables involved, numerous authors in the field of soil mechanics have wisely expressed caution in the extrapolation of the results of small-scale loading tests to the surface settlements of prototype footings. The illustrative examples given in this section seem to indicate that the use of non-dimensional parameters obtained with the methods of dimensional analysis provide a rational basis for the transformation from model studies to prototype response. Although the examples given show very good agreement with the methods of Housel, Kogler and Scheidig, and

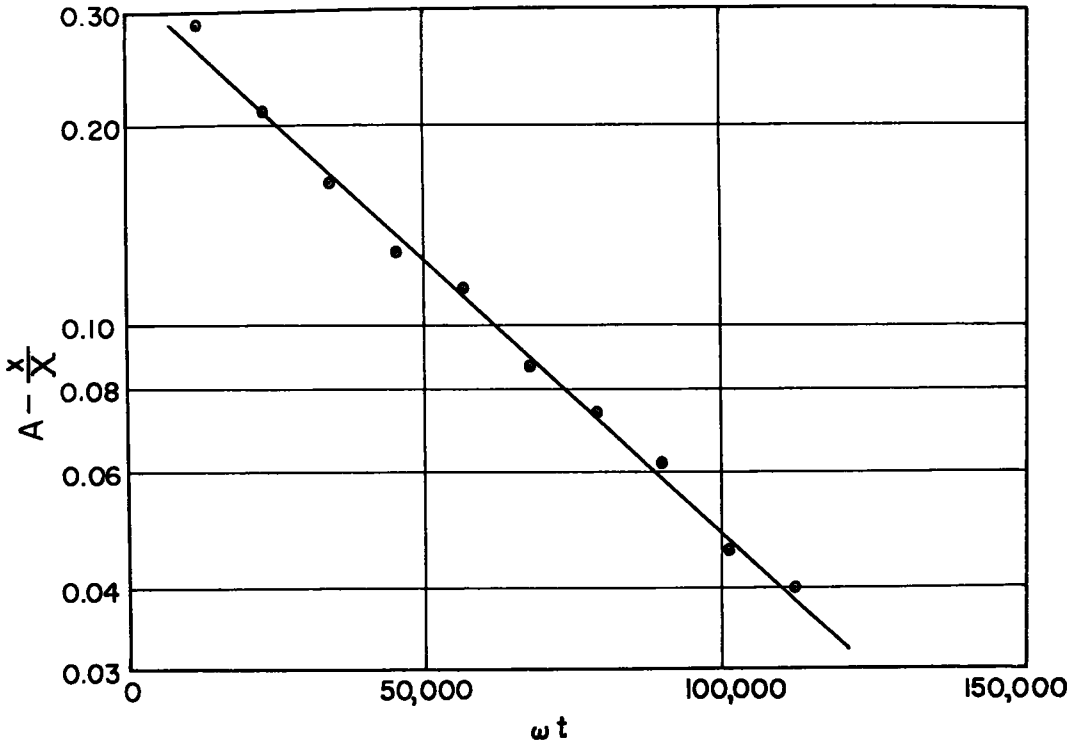


Figure 19. Semi-logarithm fit of dynamic creep data.

with some of the observations of Sowers, Taylor, Terzaghi, Tschebotarioff, Andersen, Peck, Krynine and others, the authors must caution the would-be user that the work reported in this paper is only the initial preliminary part of the study and much research is needed, particularly with regard to viscous effects, before any general quantitative results can be expressed and used with confidence.

Vibratory Tests

The vibratory experimental results presented in this section are of a qualitative nature only and no quantitative conclusions should be drawn until a more extensive research program is conducted.

Natural Frequency Tests. — In the interpretation of the non-dimensional parameters it was noted that the natural frequency of the soil-footing system is primarily a function of the magnitude and configuration of the equipment used and may be entirely different for model and prototype. Although the mechanical resonance of the system is important, the present study is more concerned with the response of vibratory loaded footings due to the basic frequency dependent properties of the soil. As a qualitative indication of field response and as a basis of comparison with the data yet to be given, the following information regarding the mechanical natural frequency is presented. The variation of the natural frequency of a circular footing with a cross-sectional area of 2.5 sq in. under a constant static force for changes in the unconfined compressive strength is given in Figure 15. The natural frequencies were obtained by measuring the free vibrations of the system as a function of time when the footing system was displaced from its equilibrium position by a small impulsive force. For the same soil type the natural frequency increases with an increase in the unconfined compressive strength. Whether, for simplicity, one considers a linear or a non-linear (soft) soil spring characteristic curve, the point value of the spring "constant" will increase with

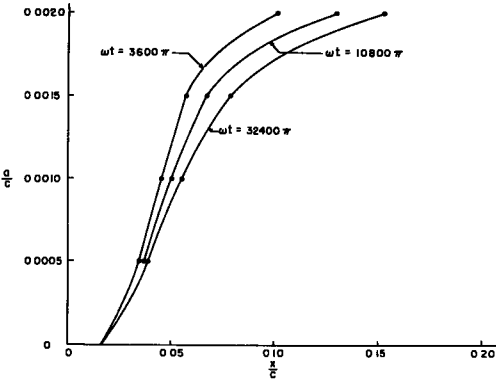


Figure 20. Sinkage parameter versus amplitude of vibration.

an increase in the unconfined compressive strength. Therefore the results of Figure 15 are to be expected. The results also agree with the increase of the compressive modulus with an increase in the compressive strength (11).

Figure 16 shows the variation of the natural frequency under different applied stresses for the same footing used in the foregoing on a hard sample (high τ) and a circular footing having area of 1.5 sq in. on a soft sample.

Figure 17 shows the variation of the natural frequency with the cross-sectional area of the footing for constant soil contact pressures on the same soil. The natural frequency decreases as the contact area increases. This agrees with the results

given by Tschebotarioff (18). Although the results of Figures 16 and 17 seem to indicate a reduction in natural frequency because of an increase in the total oscillating mass, the possibility also exists that the effective spring characteristics of the soil are non-linear and also changing. Much additional research is required before any definite conclusions can be made regarding the aforementioned variations.

In addition to these results, it was found that the size of the bin used to hold the soil for the model footing tests can affect the value of the natural frequency.

Time Effects. — Figure 18 is a typical curve of x/c versus ωt and is actually a dynamic creep test. Note the similarity between Figure 18 and the shape of curves in Figure 12. The most consistent fit of such data was obtained by plotting $\log(a - x/X)$ versus ωt , as shown in Figure 19, where X is the ultimate sinkage and A is a constant. Inasmuch as the resultant curve is approximately a straight line, the sinkage can be expressed in the form

$$x = X (A - B e^{-2.3 S \omega t}) \tag{9}$$

where B and S are the intercept and slope of the curve. For a controlled set of tests it may be possible to get A , B , S and X as functions of the other π terms. To date such an ambitious test program has not been conducted.

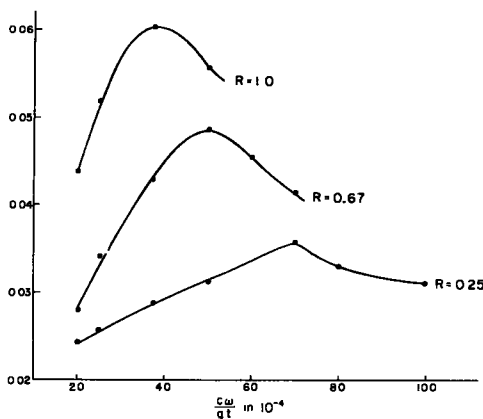


Figure 21. Sinkage parameter versus frequency parameter.

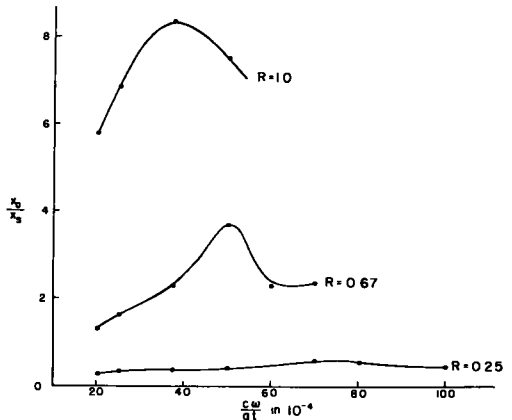


Figure 22. Sinkage ratio versus frequency parameter.

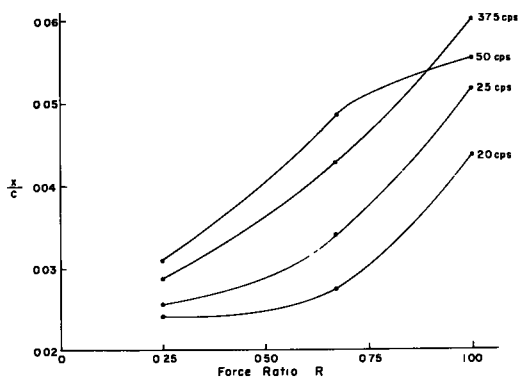


Figure 23. Sinkage parameter versus force ratio.

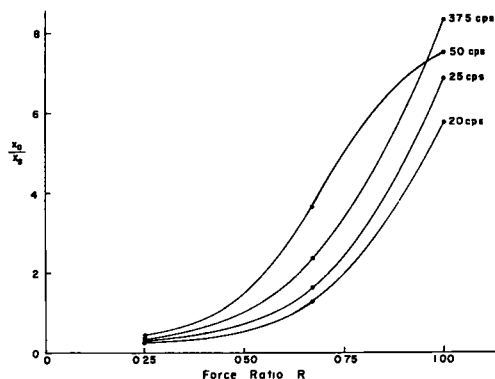


Figure 24. Sinkage ratio versus force ratio.

Amplitude Effects. — Figure 20 shows the variation of sinkage as a function of the amplitude of vibration for the same footing, static contact pressure and soil with a constant frequency of vibration at various values of ωt . The exponential increase in sinkage as a function of the amplitude agrees with the results obtained by the senior author, Kondner (11), for the vibratory unconfined compression testing of the soil being used. It must be remembered that the results of such a non-dimensional plot will change with variations in soil type and strength characteristics, frequency of vibration and magnitude of the stress level about which the stress perturbations are taking place.

Frequency and Force Ratio Effects. — The variation of the sinkage parameter (x/c) as a function of the frequency parameter ($c \omega / gt$) is presented in Figure 21 for different values of the force ratio R . The force ratio is the ratio of the dynamic to static contact stresses and its relation to the π_4 term is given by Eq. 1. These results were obtained on a soft sample with a footing having a cross-sectional area of 1.5 sq in. The total force (static plus maximum dynamic force amplitude) was kept constant for these tests. As a basis of comparison the natural frequencies of the footing for the various static stress levels used in the experiments were found by the free vibration method to be 63, 57, and 58 cycles per second for values of $R = 1.0, 0.67,$ and $0.25,$ respectively. Figure 22 is a plot of the ratio of the dynamic sinkage to the static sinkage x_D/x_S as a function of the frequency parameter for constant force (stress) ratios. The variation of x/c and x_D/x_S as functions of the force ratio for various values of the frequency are presented in Figures 23 and 24. These figures show that the sinkage parameter, frequency term and the force ratio are all interrelated. Figure 21 shows a decrease in the frequency of the peak response for an increase in the force ratio while the natural frequency data show there should have been a slight increase in the peak response frequency. Thus, the influence of the amplitude of the dynamic force on the peak response is an indication of non-linear spring and damping characteristics.

The non-linearity seems to increase with an increase in the magnitude of the dynamic force amplitude. When related to spring characteristics this indicates a "soft spring" response. This agrees with the results of the senior author's recent work on the dynamic viscoelastic properties of the soil in question (11).

Figures 21 through 24 show that the dynamic sinkage is not necessarily a mechanical resonance phenomenon but may also be a function of the frequency and stress level dependence of the soil properties. Although in many cases it is difficult to separate their effects, it is believed that the frequency and stress level dependence is more important in some cases than the mechanical resonance. Because of the limited power output of the vibratory apparatus currently being used, a wider range of force ratios and frequencies could not be studied.

FAILURE MECHANISM

The failure mechanism involved in the vibratory sinkage of rigid footings on homo-

geneous, cohesive soils is similar to that given by the senior author for the vibratory penetration of soils (12).

CONCLUSIONS

The method of dimensional analysis forms a rational basis for investigating the sinkage (surface settlement) of rigid footings on homogeneous cohesive soils under static and vibratory loads. Such a basis greatly enhances the transformation from model studies to prototype phenomena by avoiding the difficult task of model analysis.

Illustrative practical static problems have been solved using the non-dimensional method and the results were in very good agreement with the methods of analysis of Housel, Kogler and Scheidig and with some of the published observations of Sowers, Taylor, Terzaghi, Tschebotarioff, Andersen, Krynine and others.

Thus, the illustrative examples and the non-dimensional analysis of reported field data indicate that the static sinkage of rigid footings on homogeneous soils can be accurately predicted from x/c versus $F_T/A\tau$ relations as functions of c^2/A , regardless of the combination of total applied force, shape of footing and unconfined compression strength of the soil. The accuracy of the method seems to be somewhat affected by viscous time effects. These viscous effects seem to be not only a function of the soil considered, but also a function of the stress level applied to the soil. An extension of some of the tests reported, in conjunction with other rheological experiments, might possibly be used to obtain quantitative information about such phenomena.

The influence of the cross-sectional shape of the footing seems to be adequately taken into account in the non-dimensional method by the parameter c^2/A , where c is the perimeter and A the cross-sectional area of the footing. Some generalizations for relating the surface settlement and the size of footing have been obtained from the non-dimensional method and found to agree with those given by numerous authors. The senior author intends to extend the present study to include the effects of stratification, eccentricity of loading, friction between the footing and the soil, single impulse loading, and the influence of a rigid ledge below the soil mass for both cohesionless and cohesive soils. It is felt that these difficult conditions can also be handled with the methods of dimensional analysis.

The vibratory sinkage of footings is not only a function of the shape of the footing but also a function of the amplitude and frequency of vibration, the ratio of the dynamic stress to the static stress applied, and the dynamic viscosity of the soil. Although the natural frequency of the soil-footing system is important, considerable sinkage can be obtained at frequencies other than the mechanical resonance. Such response is believed to be due to the frequency and stress level dependence of soil properties. Thus, the sinkage of footings under vibratory loading is a highly non-linear problem and considerable investigation is needed before accurate predictions of field response can be made.

There is a necessity in the field of soil mechanics for more coordinated, comprehensive investigations of the rheological properties of soils both statically and dynamically. A systematic investigation should be conducted to determine the effects of moisture content, grain size distribution, mineral content, and nature of the pore water on the elasticity, anelasticity, creep and stress relaxation spectra, recovery behavior and dynamic frequency response of both cohesive and non-cohesive soils. Such studies will undoubtedly lead to a better understanding of stress-strain-time effects and hence to more rational solutions to many of the problems facing the field of soil mechanics.

ACKNOWLEDGMENT

The research reported in this paper was conducted at The Johns Hopkins University, Civil Engineering Department, and is the outgrowth of the senior author's work on the laboratory cutting, compaction and penetration of soils which is sponsored by the U. S. Army Engineer Waterways Experiment Station.

REFERENCES

- Andersen, P., "Substructure Analysis and Design." Ronald Press, New York, N. Y. (1948).

2. Ayre, R. S., and Kondner, R. L., "Laboratory Apparatus for Vibratory Cutting and Penetration of Soils, Preliminary Development." Technical Report No. 1 by The Johns Hopkins University to U.S. Army, Corps of Engineers, Waterways Experiment Station (Dec. 1957).
3. Ayre, R. S., and Kondner, R. L., "Cutting and Penetration of Soils under Vibratory Loading: A Progress Report." HRB Proc., 37:506-516 (1958).
4. Benkelman, A. C., and Williams, S., "A Cooperative Study of Structural Design of Nonrigid Pavements." HRB Special Report 46 (1959).
5. Benkelman, A. C., and Olmstead, F. R., "A Cooperative Study of Structural Design of Nonrigid Pavements." Public Roads, 25: 2 (Dec. 1947).
6. Cowin, S. C., Kondner, R. L., and Ayre, R. S., "Bibliography Relating to Vibratory Cutting, Penetration and Compaction of Soils." Technical Report No. 2, by The Johns Hopkins University to U.S. Army, Corps of Engineers, Waterways Experiment Station (Jan. 1958).
7. Cowin, S. C., Kondner, R. L., and Ayre, R. S., "Bibliography Relating to Vibratory Cutting, Penetration and Compaction of Soils." (Supplement No. 1), Technical Report No. 3 by The Johns Hopkins University to U.S. Army, Corps of Engineers, Waterways Experiment Station (Feb. 1958).
8. Cowin, S. C., Kondner, R. L., and Ayre, R. S., "A Critical Review of Selected Literature Relating to the Vibratory Cutting, Penetration and Compaction of Soils." Technical Report No. 4 by The Johns Hopkins University to U.S. Army, Corps of Engineers, Waterways Experiment Station (April 1958).
9. Kondner, R. L., Ayre, R. S., and Chae, Y. S., "Laboratory Investigation of the Vibratory Cutting and Penetration of Soils (Part I)." Technical Report No. 5, by The Johns Hopkins University to U.S. Army, Corps of Engineers, Waterways Experiment Station (June 1958).
10. Kondner, R. L., and Ayre, R. S., "Study of Vibratory Cutting, Penetration and Compaction of Soils." Technical Report No. 6 by The Johns Hopkins University to U.S. Army, Corps of Engineers, Waterways Experiment Station (June 1958).
11. Kondner, R. L., "The Vibratory Cutting, Compaction and Penetration of Soils." Technical Report No. 7 by The Johns Hopkins University to U.S. Army, Corps of Engineers, Waterways Experiment Station (July 1959).
12. Kondner, R. L., and Edwards, R. J., "The Static and Vibratory Cutting and Penetration of Soils." HRB Proc., 39:583-604 (1960).
13. Krynine, D. P., "Soil Mechanics." McGraw-Hill, New York (1947).
14. Sowers, G. B., and Sowers, G. F., "Introductory Soil Mechanics and Foundations." Macmillan Co., New York (1951).
15. Taylor, D. W., "Fundamentals of Soil Mechanics." John Wiley, Chapter 19 (1948).
16. Terzaghi, K., "Theoretical Soil Mechanics," John Wiley and Sons, p. 401, New York (1943).
17. Terzaghi, K., and Peck, R. B., "Soil Mechanics in Engineering Practice." John Wiley and Sons, New York (1948).
18. Tschebotarioff, G. P., "Soil Mechanics, Foundations, and Earth Structures." McGraw-Hill, Chapters 9 and 18 (1951).